

- (360) J. W. Daly, M. Huang, and H. Shimizu, in "Advances in Cyclic Nucleotide Research," vol. 1, P. Greengard, R. Paoletti, and G. A. Robison, Eds., Raven, New York, N.Y., 1972, p. 375.
- (361) P. Uzunov and B. Weiss, in "Advances in Cyclic Nucleotide Research," vol. 1, P. Greengard, R. Paoletti, and G. A. Robison, Eds., Raven, New York, N.Y., 1972, p. 435.
- (362) S. Kakiuchi, R. Yamazaki, and Y. Teshima, in "Advances in Cyclic Nucleotide Research," vol. 1, P. Greengard, R. Paoletti, and G. A. Robison, Eds., Raven, New York, N.Y., 1972, p. 455.
- (363) D. N. Harris and M. B. Phillips, in "Abstracts of the 5th International Congress on Pharmacology, San Francisco, July 23-28," 1972, p. 96.
- (364) E. W. Salzman, *N. Engl. J. Med.*, **286**, 358(1972).
- (365) M. C. Rosenberg and C. M. Walker, *Brit. J. Haematol.*, **24**, 409(1973).
- (366) J. H. Jones, W. J. Holtz, and E. J. Cragoe, Jr., *J. Med. Chem.*, **16**, 537(1973).
- (367) T. Novinson, R. Hanson, K. Dimmitt, L. N. Simon, R. K. Robins, and D. E. O'Brien, in "Fifth International Congress on Pharmacology, July 23-28," 1972, p. 169.
- (368) T. Novinson, M. Scholten, L. N. Simon, R. K. Robins, and D. E. O'Brien, *Amer. Chem. Soc., Div. Med. Chem., 164th ACS Nat. Mtg., New York, N.Y., Aug. 28-31*, 52(1972).
- (369) T. Novinson, R. H. Springer, K. Dimmitt, M. Scholten, L. N. Simon, R. K. Robins, and D. E. O'Brien, *ibid.*, 54(1972).
- (370) R. H. Springer, M. Scholten, L. N. Simon, R. K. Robins, and D. E. O'Brien, *ibid.*, 53(1972).
- (371) J. Kobe, R. H. Springer, M. Scholten, J. Miller, L. N. Simon, R. K. Robins, and D. E. O'Brien, *ibid.*, 55(1972).
- (372) M. W. Nott, *Brit. J. Pharmacol.*, **42**, 666P(1971).
- (373) G. E. Davies, F. L. Rose, and A. R. Somerville, *Nature New Biol.*, **234**, 50(1971).
- (374) R. E. Nitz, E. Schraven, and D. Trottnow, *Experientia*, **24**, 334(1968).
- (375) K. P. Kupiecki, *J. Lipid Res.*, **14**, 250(1973).
- (376) A. W. Gomoll and C. J. Sloan, *Life Sci.*, **13**, 7199(1973).
- (377) J. Miller, M. Scholten, J. Kobe, R. Springer, D. O'Brien, R. Robins, and L. Simon, *164th ACS Nat. Mtg., New York, N.Y., Aug. 28-31*, 56(1972).
- (378) E. N. Ramsden, *Biochem. J.*, **120**, 12P(1970).
- (379) P. F. Gulyassy, *Life Sci.*, **10**, 451(1971).
- (380) A. Lucacchini, U. Montali, M. Ranieri, and C. A. Rossi, *B. Soc. Ital. Biol. Sp.*, **48**, 17(1972).
- (381) J. I. Davies, *Nature*, **218**, 349(1968).
- (382) M. M. Appleman and R. G. Kemp, *Biochem. Biophys. Res. Commun.*, **24**, 564(1966).
- (383) D. G. Peers and J. I. Davies, *Biochem. J.*, **124**, 8P(1971).
- (384) J. N. Fain, R. H. Pointer, and W. F. Ward, *J. Biol. Chem.*, **247**, 6866(1972).

ACKNOWLEDGMENTS AND ADDRESSES

Received from *Mead Johnson Research Center, Mead Johnson & Company, Evansville, IN 47721*

The authors acknowledge the contribution of those who supplied manuscripts in press. The expert assistance of Mrs. S. Graves and Mrs. J. Parks in typing the manuscript and arranging the references is also gratefully acknowledged.

* To whom inquiries should be directed.

RESEARCH ARTICLES

Decomposition of *p*-Aminosalicylic Acid in the Solid State

J. T. CARSTENSEN* and PAKDEE POTHISIRI

Abstract □ Aminosalicylic acid was used as a test substance to show that a solid-state decomposition governed by nucleation kinetics can give rise to first-order kinetics. The effect of sorbed moisture at a low degree of coverage was tested. Sorbed moisture theories proposed previously apply when it is realized that the rate constants in the presence of the sorbed layer may differ from the values of these parameters under anhydrous conditions.

Keyphrases □ Decomposition—aminosalicylic acid in solid state giving rise to first-order kinetics, sorbed moisture theories discussed □ Aminosalicylic acid—decomposition in the solid state, first-order decomposition patterns □ Stability—decomposition of aminosalicylic acid in solid state, sorbed moisture theories discussed, first-order decomposition patterns □ Moisture—decomposition of aminosalicylic acid in solid state

The problems of stability of solid dosage forms have been discussed, although not with great frequency, in the pharmaceutical literature. Reference

is made in this report to two basic articles (1, 2). For more complete references, the reader is referred to reviews on the subject (3, 4).

The problem of how to extrapolate pharmaceutical stability data is of importance in excess determination and in label statements on expiration dating; to this end, it is necessary to know prior to extrapolation [or to determine from the data (5)] if the decomposition is zero or first order.

The stability of the drug without excipients and the stability of the drug in the presence of moisture (6) (but no other excipients) throw some light on the theoretical order of reaction and the actual mode of decomposition. In the absence of moisture, topochemical- and nucleation-governed reactions occur (3, 7, 8); of these, *some* topochemical patterns may be approximated by first-order decay (3, 9). In the absence of moisture, the more common decomposition

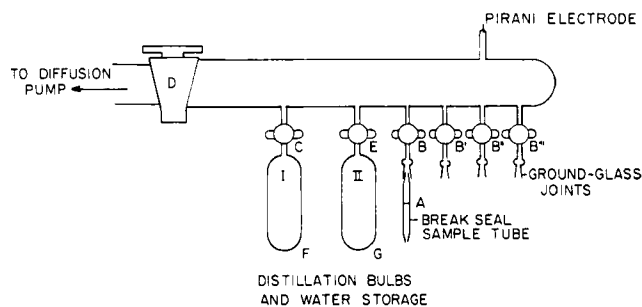


Figure 1—Vacuum manifold used in the study.

pattern is governed by nucleation (7, 8), giving rise to sigmoid curves which should not be simple first or zero order.

In the presence of moisture, a simple, sorbed moisture theory (1, 2) would view the moisture present as a "bulk" saturated solution of the drug in the sorbed water; therefore, the decomposition kinetics should be dictated by the rates in saturated solution and be zero order. In the decomposition of aspirin, Leeson and Mattocks (1) found this to be the case (when pH effects were accounted for). Kornblum and Sciarrone (2) found that when moisture is present in the solid-state decomposition of aminosalicic acid, decomposition rates are increased; in this case, however, the decomposition rates differed from those predicted by solubility.

A recent publication (3) gave tentative explanations why, theoretically, a solid could (in the absence of other ingredients) decompose in a pseudo-first-order fashion. With the presence of moisture, reaction orders should tend toward zero order if the system is considered to consist of solid plus bulk sorbed saturated moisture layer (after pH effects are accounted for).

The intent of this article is to show that first-order decomposition patterns may be tenable both (a) in the absence of moisture and (b) when moisture coverage is low. This latter feature, of course, brings the model system (aminosalicylic acid) close to the situation encountered in dosage forms. In achieving this objective, the findings of previous investigators (1, 2) will be confirmed.

EXPERIMENTAL AND RESULTS

p-Aminosalicylic acid was recrystallized from ethanol, dried *in vacuo*, ground in a mortar, and redried. The specific surface area

Table I—Constant-Temperature Baths for Controlled Water Vapor Pressure

Substance in Dewar Jar	Temperature	Water Vapor Pressure, torr
Water ^a	3.5°	5.9
Solid-liquid Benzene ^b	6.8°	7.4
Solid-liquid <i>p</i> -xylene ^b	13.2°	11.38
Water ^a	20°	17.56
Water ^a	25°	23.76

^a This temperature is equal to the controlled air temperature. ^b This is a "slush" produced by adding liquid nitrogen to the benzene (xylene) in a Dewar jar; it produces a temperature of the melting point of benzene (xylene) as long as both solid and liquid benzene (xylene) are present.

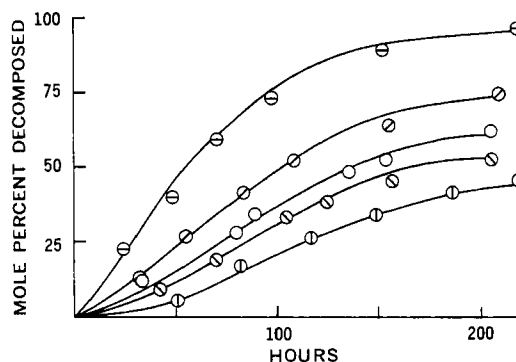


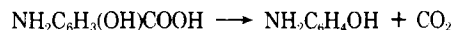
Figure 2—Solid-state decomposition of aminosalicic acid at 65° in the presence of moisture. Key: ○, 5.9 torr; □, 7.4 torr; △, 11.4 torr; ◇, 17.6 torr; and ▽, 23.8 torr.

of the powder was 0.36 m²/g, as determined by Brunauer, Emmett, and Teller (BET) nitrogen adsorption (10).

Samples were prepared in breakseal tubes *in vacuo* on a high vacuum rack as described previously (11). A schematic drawing of the high vacuum manifold is shown in Fig. 1. The aminosalicic acid was placed in the breakseal tube at point A. Water was placed in the distillation bulb I at point F. All stopcocks except for D were then closed, and the system was evacuated thoroughly (<0.5 mtorr). Stopcocks C and E were then opened and D was closed; liquid nitrogen was placed in a Dewar flask around G, and the water was distilled into distillation bulb II. Stopcock D was opened, the system was evacuated, D was closed, and the process was repeated with liquid nitrogen at point F. This distillation and evacuation process was carried out (four times) until lack of measurable pressure after a distillation on the Pirani gauge at H showed the water to be completely deaerated.

A constant-temperature bath was then placed at F and (with D and E closed) B was opened. In this manner, the aminosalicic acid is exposed to a water vapor pressure dictated by the temperature of the constant-temperature bath at F. The types of constant-temperature baths used are listed in Table I. Stopcock C was occasionally closed; if the pressure measured on the Pirani gauge dropped, then equilibrium had not yet been achieved. At the point in time when the pressure no longer dropped, B and C were both closed, and the breakseal tube was removed by sealing it off by flame. Four samples could be prepared at a time (Fig. 1). A series was also prepared without moisture present.

The sealed tubes were stored at 60 ± 0.5° for the periods of time indicated in Fig. 2. After storage, the carbon dioxide evolved was determined manometrically as described by Musa (12), except a cold finger in the system was cooled to -5° to allow condensation of water without affecting the carbon dioxide pressure. Each sample was checked titrimetrically, and the decomposition was shown to be the straightforward, stoichiometric decarboxylation shown in Scheme I.



Scheme I

The results are shown in Fig. 2 and are tabulated in Table II.

The results from the series performed without the presence of moisture are shown in Fig. 3. Several temperatures were used.

Knowledge of the solubility of aminosalicic acid is needed for

Table II—Decomposition Rate Constants of Aminosalicic Acid in Presence of Moisture

Vapor Pressure, P, torr	Log P	Apparent Decomposition Rate Constant, ζ hr ⁻¹ (Eq. 18)
5.9	0.77	0.0031
7.4	0.87	0.0035
11.4	1.06	0.0045
17.6	1.25	0.0068
23.8	1.38	0.0088

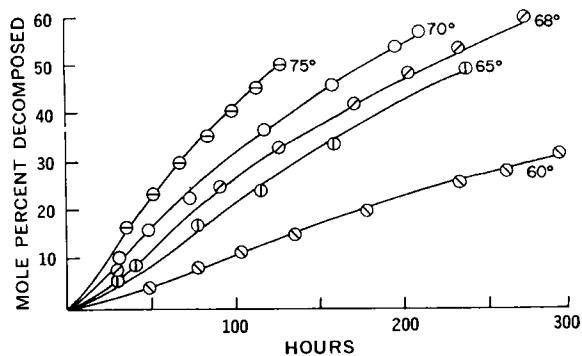


Figure 3—Solid-state decomposition of aminosalicic acid at various temperatures. Key: \ominus , 75°; \circ , 70°; \diamond , 68°; \square , 65°; and \circ , 60°.

the analysis of the solid kinetic data where moisture is present. Forty grams of aminosalicic acid was stored with 50 g of water in an erlenmeyer flask closed with a U-tube water trap at 65°. Samples of supernate were assayed spectrophotometrically at 300 and 230 nm (2) at various times. The contents of aminosalicic acid and of *m*-aminophenol as a function of time are shown in Fig. 4.

The final composition approaches 2.6 moles (278 g) of *m*-aminophenol and 0.52 mole (80 g) of aminosalicic acid per kilogram sample, i.e., the solubility of aminosalicic acid at 65° is 0.52 mole/642 g of water or 0.81 mole/kg of water. An order of magnitude estimation of the decomposition rate constant of aminosalicic acid in solution can be made via $dC/dt = -k_2C$, i.e., $k_2 = -(1/C) dC/dt$ in the following fashion. The first point on the aminosalicic acid curve in Fig. 4 is 0.27 at 4 hr; so in the first 4 hr, C is 0.27 (or less). The first point on the *m*-aminophenol curve is 1.23, so that dC/dt is at least $1.23/4 = 0.308$, so that k_2 is at least $k_2 = (1/0.27) 0.308 = 1.14 \text{ hr}^{-1}$. This compares fairly favorably with the value of 0.95 hr^{-1} , which will be referred to later.

To estimate the amount of moisture present as sorbed moisture on the solid itself, it is necessary to determine the moisture isotherm of the solid. This was done using the apparatus arrangement shown in Fig. 5 for determination of the isotherm at room temperature ($27 \pm 0.2^\circ$). All parts of the apparatus are Pyrex glass and all stopcocks are either vacuum stopcocks or hollow capillary stopcocks. The system was fused (by oxygen-gas flame) and all volumes were determined by helium gas expansion (10, 15).

Water was placed in the distillation bulb H and purified by repeated distillation between H' and H as described earlier. Aminosalicic acid was placed in the sample tube at J; all stopcocks were opened, and the system was thoroughly evacuated and the stopcocks were then closed. The mercury level in the McLeod gauge was then raised to the highest calibration mark (L).

Stopcocks C and F were then opened and the capillary space was

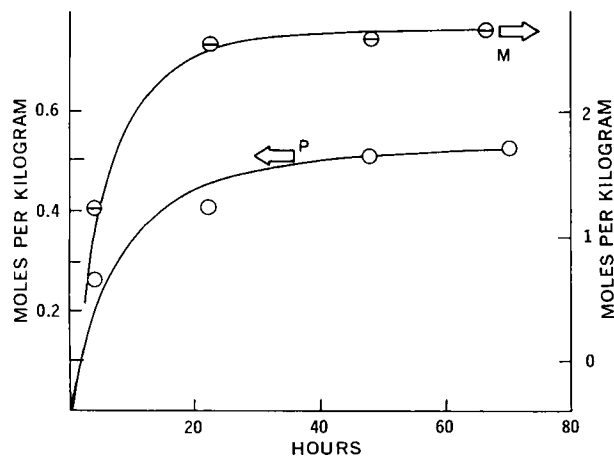


Figure 4—Contents of aminosalicic acid (P) and *m*-aminophenol (M) of aminosalicic acid stored at 65° as a function of time. Key: \circ , aminosalicic acid; and \ominus , *m*-aminophenol.

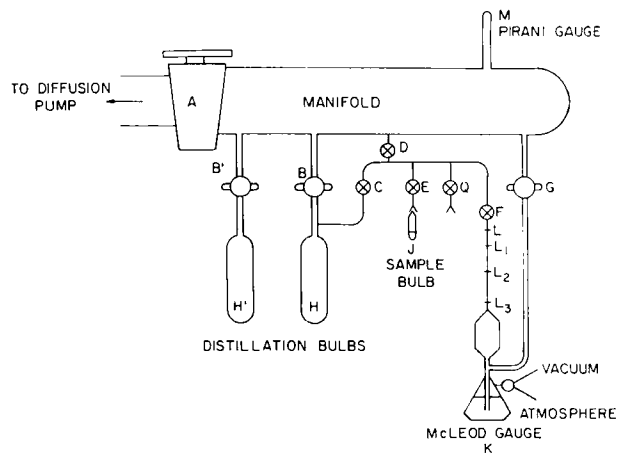


Figure 5—Vacuum setup for determination of isotherms at room temperature.

saturated with water vapor (4 hr), so the space between C and L would exhibit a water vapor pressure of 26.7 torr (saturation pressure of water at 27°) as registered on the McLeod gauge. Stopcock C was then closed and stopcock E was opened, and the vapor expanded into the head space over the sample.

Knowledge of the volume before and after the expansion permits calculation of the theoretical pressure (P_t) after opening stopcock E. The actual pressure (P) was measured on the McLeod gauge and was smaller than the theoretical. The difference ($\Delta P = P_t - P$) was converted into the number of moles of water, and this figure was divided by the number of moles of aminosalicic acid in the sample to give the adsorbed amount (x) in moles per mole at equilibrium pressure P . The mercury level was then lowered to L_2 , giving a new set of values for P_t , P , and x ; a series of such values (giving the isotherm at 27°) is shown graphically in Fig. 6. A similar isotherm was performed for *m*-aminophenol.

The moisture isotherm at 60° presented a greater problem experimentally. The apparatus and approach outlined in Fig. 7 were used. A closed-end manometer with a side arm (EF) was made and fused onto ground-glass joints (A and B), and the manometer was loaded with mercury to the level shown. A sample of aminosalicic acid was then placed in the noncapillary end of a breakseal tube;

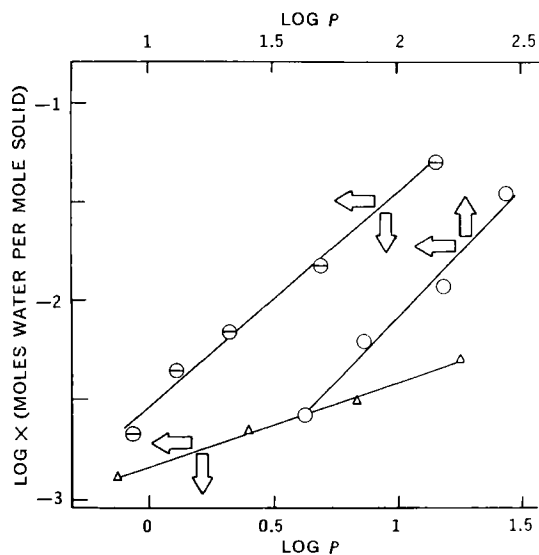


Figure 6—Langmuir plots of moisture isotherms of aminosalicic acid at 25° (\odot) and 65° (\circ) and of *m*-aminophenol at 25° (Δ). The least-squares fit equations are: aminosalicic acid at 25°, $\log x = 1.10 \log P - 2.05$; aminosalicic acid at 65°, $\log x = 1.31 \log P - 3.90$; and *m*-aminophenol at 25°, $\log x = 0.33 \log P - 2.77$.

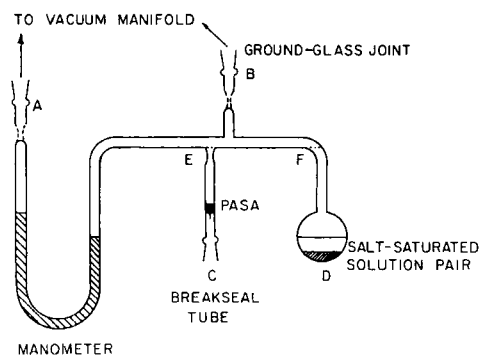


Figure 7—Apparatus for determination of isotherms at 65°.

this tube was fused onto the side arm at E and a bulb of water (D) was fused onto the side arm at F.

The assembly was then attached to a high vacuum rack at A and B (and checked for tightness with a Tesla coil). After evacuation the apparatus was sealed with an oxygen-gas flame at A and B, and the breakseal tube was narrowed down at E. The entire apparatus was then placed in a 60° oven¹ and, after equilibrium had been obtained (as ascertained by the mercury level being constant), the breakseal tube was sealed off with an oxygen-gas flame while the apparatus was still in the constant-temperature oven.

The breakseal tube was then inverted and attached to the vacuum rack at ground-glass joint Q (Fig. 5), and the total amount of water in the sample was determined on the McLeod gauge. Four salt-saturated solution pairs were used, producing the pressures shown in Table III.

For reasons that shall become apparent in the Discussion section, the effect of the size of the reaction vessel was investigated. The sample holder in most of this study had a volume of 7 ml. A kinetic study was performed at 65° with sample holders of 20 and 40 ml. The results are shown in Fig. 8.

The effect of oxygen on the decomposition was studied by exposing the aminosalicic acid sample to 50 torr pressure of oxygen prior to sealing off the sample holder and storing it at 65°. The oxygen was prepared from potassium permanganate and manganese dioxide by the method of Sanderson (16). The results are shown in Fig. 8.

The effect of saturating the atmosphere above the aminosalicic acid sample with mercury vapor was studied by blowing a side arm onto the sample holder and depositing a drop of mercury in the side arm. The holder was kept in an upright position during the decomposition so that there would be no contact between liq-

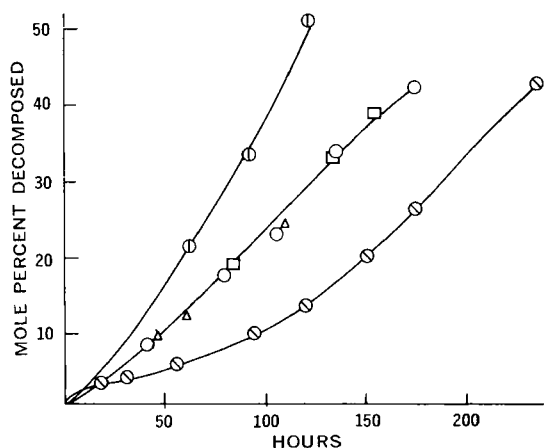


Figure 8—Decomposition of aminosalicic acid at 65°. Key: \odot , in an atmosphere of saturated mercury vapor; \circ , in an atmosphere of 50 torr pressure of oxygen; \triangle , in vacuo with a 7-ml sample holder; \square , in vacuo with a 40-ml sample holder.

¹ Model 1302, Hotpack Corp., Philadelphia, PA 19135

Table III—Salts Used in Contact with Their Saturated Solutions at 65° for Moisture Isotherms

Equilibrium Water Vapor Pressure at 65°, P, torr	Salt	Log P
148	MgSO ₄	2.17
104	LiCl	2.02
44	MgCl ₂ ·6H ₂ O	1.64
26	CaCl ₂ ·2H ₂ O	1.41

uid mercury and the solid sample during this period. The results are shown in Fig. 8.

The surface area of a series of samples was determined by BET nitrogen adsorption as described previously (10). The samples were stored for various times at 65°, and the surface area then was determined again. The results are shown in Table IV.

DISCUSSION

The decomposition of aminosalicic acid in the solid state is a so-called Type I solid reaction—*viz.*, one where 1 mole of solid decomposes into 1 (or more) mole of a solid decomposition product and 1 (or more) mole of a gas (17). In Type I reactions, the decompositions are governed by strains in the crystal, induced by the formation of product molecules; this is referred to as nucleation (18, 19). As the strain increases, the original crystal may crack and form new surfaces upon which further decomposition can occur. Formation of the product molecules appears, at first, in the form of nuclei which are mainly located on the surface (18) or (rarely) inside the crystal (19).

Occurrence of the nuclei in rows suggests that they are confined to lines of strain in the crystal. Initiation of decomposition appears at the surface, but the decomposition progresses by two routes: (a) along the surface itself, and (b) by penetration into the crystal. An accepted and frequently substantiated theoretical model for such a decomposition mechanism is the model of Prout and Tompkins (7, 8). They assumed that there initially are N^* potential (energetic) sites for nucleation (dislocations, vacancies, surface steps, etc.) and that the nucleation rate is proportional to N , the number of nuclei present at time t ; *i.e.*, $dN/dt = (\alpha)(N)$. The term α is a propagation probability; but at a certain point in the decomposition, the rows of nuclei start merging, so that there also is a termination probability, β , associated with the decomposition. This is expressed in the form:

$$dN/dt = [\alpha - \beta](N) \quad (\text{Eq. 1})$$

This cannot be integrated directly, since α and β are functions of time.

Most decompositions of Type I are sigmoid-shaped curves when decomposition is plotted *versus* time. Prout and Tompkins (7) noted that the inflection point usually occurs at $x = 0.5$ and reasoned that α must equal β at this point; they further assumed that $\beta = 0$ when $t = 0$ ($x = 0$) so that α and β could be interrelated by a function such as:

$$\beta = 2x\alpha \quad (\text{Eq. 2})$$

This makes β zero at time zero and $\alpha = \beta$ at the inflection point.

Table IV—Surface Area of Aminosalicic Acid Samples after Storage at 65°

Time, t, hr	Fraction, x, Decomposed	Surface Area, A, in m ² /g	Increase in Area, ΔA	$0.003t + \ln(\Delta A)$	$\ln t - 40$	$\ln(t - 40)$
0	—	0.36	—	—	—	—
45	0.07	1.73	1.37	0.45	5	1.61
65	0.11	3.79	3.43	1.43	25	3.22
100	0.18	6.45	6.09	2.11	60	4.09
138	0.24	9.20	8.84	2.59	98	4.58

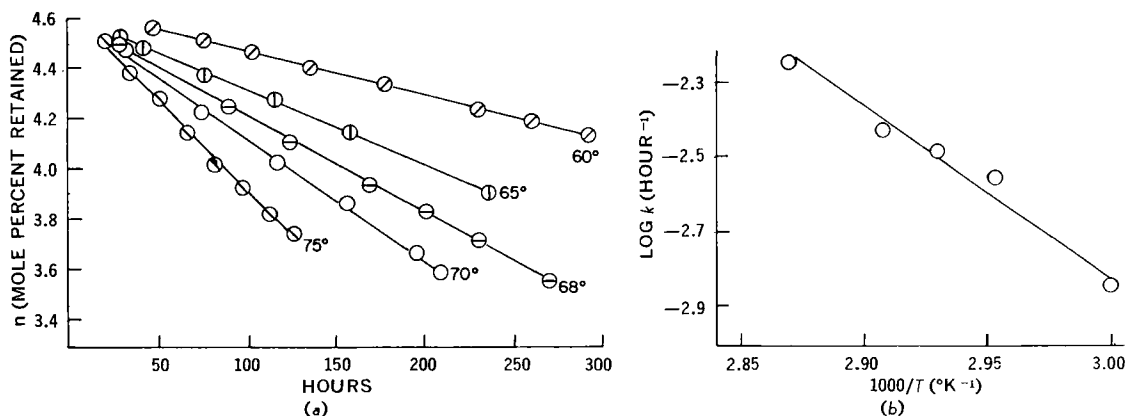


Figure 9—(a) Data from Fig. 3 plotted according to Eq. 12. (b) Arrhenius plot of data from Fig. 9a.

This reasoning is, of course, based on boundary conditions, and many functions [e.g., $\beta = (2x)^2(\alpha)$] would satisfy the stated requirements as well.

Implementation of Eq. 2 and the assumption that:

$$dx/dt = k'N \quad (\text{Eq. 3})$$

has been shown (7) to lead to the sigmoid-shaped curve:

$$x/(1-x) = \exp[k'(t-t_i)] \quad (\text{Eq. 4})$$

where t_i is the time at which the inflection point ($x = 0.5$) occurs.

It is noted from Fig. 3 that it is not justified, in the case reported here, to assume that the inflection point occurs at $x = 0.5$. An approach similar to the one used by Prout and Tompkins is therefore developed in the following section.

If a method existed for measuring N , it would be possible to test Eq. 1 directly. If one assumes that N is proportional to the increase in BET surface area, then such a method exists and this, indeed, is the purpose of following the BET surface area experimentally as a function of time (Table IV). In place of the assumptions made by Prout and Tompkins for α and β , it is assumed here that nucleation starts at some time t_0 (which is assumed to be larger than zero) with a propagation probability $\alpha_0 (<1)$ and that (as in the Prout-Tompkins treatment) $\alpha = \beta$ at $t = t_i$. At infinite time, the termination probability is $\beta = \beta_0$. A function that meets these requirements is:

$$\alpha - \beta = \frac{(\alpha_0 + \beta_0)(t_0 - q)}{t - q} - \beta_0 \quad (\text{Eq. 5})$$

where:

$$q = \frac{(\alpha_0 + \beta_0)t_0 - \beta_0 t_i}{\alpha_0} \quad (\text{Eq. 6})$$

Equation 6 may be rearranged to $\alpha_0(q - t_0) = \beta_0(t_0 - t_i)$; and

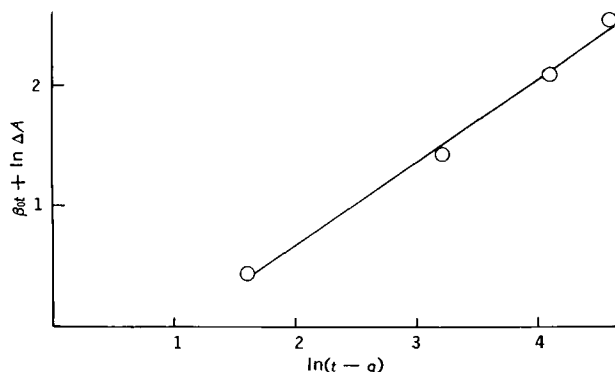


Figure 10—Data from Table IV treated by Eq. 13 with $q = 40$.

since $t_0 - t_i < 0$, it follows that $q - t_0$ also is smaller than zero, i.e., $t_0 > q > 0$.

Equation 6 inserted into Eq. 1 yields:

$$\frac{dN}{N} = \left(\frac{(\alpha_0 + \beta_0)(t_0 - q)}{t - q} - \beta_0 \right) dt \quad (\text{Eq. 7})$$

which is integrated to:

$$\ln N = (\alpha_0 + \beta_0)(t_0 - q) \ln(t - q) - \beta_0 t + \ln Q \quad (\text{Eq. 8})$$

where $\ln Q$ is an integration constant. The nonlogarithmic form of this equation is:

$$N = Q(t - q)^{(\alpha_0 + \beta_0)(t_0 - q)} e^{-\beta_0 t} \quad (\text{Eq. 9})$$

which, inserted into Eq. 3, yields:

$$\frac{dx}{dt} = k'Q(t - q)^{(\alpha_0 + \beta_0)(t_0 - q)} e^{-\beta_0 t} \quad (\text{Eq. 10})$$

If $t_0 - q$ is small, then Eq. 10 takes the form:

$$\frac{dx}{dt} = k'Qe^{-\beta_0 t} \quad (\text{Eq. 11})$$

This is integrated to:

$$\begin{aligned} x &= 1 - e^{-\beta_0(t-t_0)} & t \geq t_0 \\ x &= 0 & t < t_0 \end{aligned} \quad (\text{Eq. 12})$$

The initial condition that $x = 0$ for $t < t_0$ has been invoked in going from Eq. 11 to Eq. 12 as has the boundary condition that $x = 1$ for $t \rightarrow \infty$; this latter implies that $k'(Q/\beta_0) = 1$. Equation 12 is a first-order expression. When t_0 is not close to q , then the expressions become more complicated. The treatment for this case is detailed in the Appendix. Data treated according to first-order presentation are graphed in Fig. 9a, and the slopes (β_0) are treated by Arrhenius plotting in Fig. 9b. The fits are good; β_0 at 65° is 0.003 hr^{-1} .

If the increase in surface area during decomposition is propor-

Table V—Amounts of Moisture Adsorbed on the Samples Studied for Decomposition

P, torr	x (Fig. 6), moles Water/mole Amino-salicylic Acid	V × 10 ³ , liters Water/mole Amino-salicylic Acid
5.9	0.063	1.14
7.4	0.081	1.46
11.4	0.131	2.36
17.6	0.211	3.80
23.8	0.294	5.30

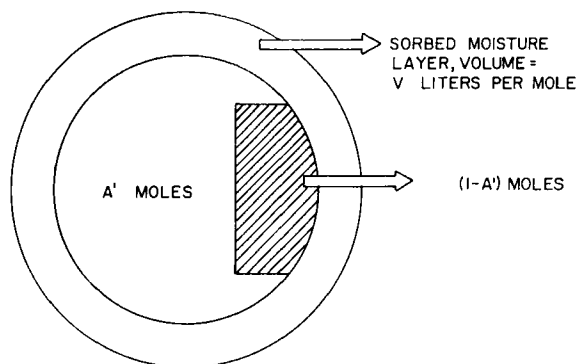


Figure 11—Schematic drawing of the proposed model.

tional to N , i.e., $\Delta A = \lambda N$, then Eq. 8 becomes:

$$\ln(\Delta A) + \beta_0 t = (\alpha_0 + \beta_0)(t_0 - q) \ln(t - q) + \ln(Q/\lambda) \quad (\text{Eq. 13})$$

The data in Table III were plotted in Fig. 10, using $\beta_0 = 0.003 \text{ hr}^{-1}$ and various values of q . The value $q = 40$ was found to linearize the surface area data best according to Eq. 13.

Although Prout and Tompkins (7) and Prout and Herley (8) found Eq. 4 to hold up to $x = 0.1$, they had to assume that the propagation constant had a form of k/t in the accelerative period; this then is an assumption over and above the ones stated. The amount and severity of assumptions made in the development of Eq. 12 are less. Once the order of reaction is established, the data reported here can be compared with data reported by other investigators (2, 20). The data are compared in the form $k = k_0 \exp(-E_a/RT)$, where E_a is the activation energy, R is the gas constant, and T is the absolute temperature.

From Ref. 20.

$$k = 4.3 \times 10^{14} \exp(-20,500/RT) \quad (\text{Eq. 14a})$$

From Ref. 2:

$$k = 6.3 \times 10^{25} \exp(-41,000/RT) \quad (\text{Eq. 14b})$$

And from this study:

$$\beta_0 = k = 3.2 \times 10^{10} \exp(-30,300/RT) \quad (\text{Eq. 14c})$$

Although these expressions seem to differ to a substantial degree, the differences are not as great as the numbers in the equations would imply at first glance. For instance, 1 mole stored for 1 hr at 80° would show 0.986, 0.995, and 0.992 mole remaining by Eqs. 14a, 14b, and 14c, respectively.

It is instructive, however, to seek the cause of the differences. The data by Sheinker and Persyanova (20) were generated in an atmosphere saturated with mercury vapor. Mercury has a vapor pressure of 0.07 and 0.2 torr at 75° and 90° , respectively; these are the principal temperatures of their study. The results obtained in the study reported here (Fig. 8) show that mercury vapor accelerates the decomposition of aminosalicic acid and this constitutes one explanation why the rate constants of Ref. 20 in general are higher than the rate constants reported here. Their reaction vessel

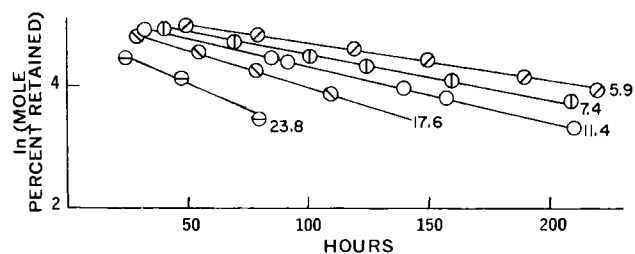


Figure 12—Data from Fig. 2 plotted by Eq. 18.

was (presumably) considerably larger than the one used here but, as shown in Fig. 8, this should not matter.

To find an explanation for the difference between the data of Kornblum and Sciarrone (2) and the results from this study, it should be noted that the former was not carried out *in vacuo*, i.e., atmospheric oxygen and nitrogen were present in the headspace. For this reason, a study was carried out here with oxygen in the sample holder headspace.

Ermer (21) and Thoma (22) studied the decomposition of aminosalicic acid in solution in the presence of oxygen and found a definite effect as compared to studies in the absence of oxygen. If there, indeed, is an oxidative effect, then the reaction rate would be expected to increase. The decomposition of solid aminosalicic acid in the presence of oxygen (Fig. 8) does, surprisingly, not imply a straightforward increase in reaction rate but rather a rapid initial rate followed by a somewhat decreased rate in the accelerative period. The reason for this is not quite clear, but the following explanation may be feasible, although no attempts to substantiate the individual points are made here.

The rapid initial rate may be a result of an oxidative reaction of the molecules on the surface; eventually the particles are completely covered by the oxidation product, and this may retard the propagation rate and cause the subsequent decrease in reaction rate. The point is that the oxidative interference with the actual decomposition explains the small difference between the data by Kornblum and Sciarrone (2) and the data in this study. By virtue of some air being present, the experimental setup by Kornblum and Sciarrone is closer to real pharmaceutical systems than the model study reported here.

Leeson and Mattocks (1), in their work on aspirin decomposition, showed that in the presence of moisture the decomposition of the solid can be accounted for by considering the adsorbed moisture as a saturated aspirin solution. The aspirin decomposes in solution with a first-order rate constant, k'' , and has a solubility of S . Knowing the volume, V , of moisture adsorbed allows calculation of a loss figure, and this value was found to be very close to the experimentally determined value.

Contrary to this, Kornblum and Sciarrone (2) found that for aminosalicic acid, using a decomposition rate constant in solution of $k_2 = 1.986 \text{ hr}^{-1}$ (21), a sorbed moisture theory would lead to the conclusion that 80% of the solid would be in solution, a fact not substantiated by visual observation. The conclusion is based on the rate constants determined in solution by Ermer (21); even though better values for k_2 (differing from Ermer's by a factor of two) have been reported (23) subsequent to the appearance of the study by Kornblum and Sciarrone, their conclusion still remains valid. Kornblum and Sciarrone did not quantitate the amounts of moisture adsorbed and hence had to refrain from quantitating their observation. The work reported here attempts to accomplish this.

If the volume of moisture adsorbed on the solid follows a Freundlich moisture isotherm, as implied by Fig. 6, then:

$$x = K(P^{1/n}) \quad (\text{Eq. 15})$$

or:

$$V = x/55.5 = K(P^{1/n}) \quad (\text{Eq. 16})$$

where K and n are Freundlich parameters, x is moles of water adsorbed per mole of aminosalicic acid, and V is kilograms of water adsorbed per mole of aminosalicic acid.

The vapor pressures used in Table I (Fig. 2) can be converted to amount of moisture adsorbed by the equations shown in Fig. 6, and these values are shown in Table V. The samples used in the kinetic study at 65° are prepared at 25° and therefore are heated from 298 to 338°K . The samples are 0.3-g samples in a 7-ml tube. It can be shown by gas law application that, at the lowest pressure, at most 4.6×10^{-7} mole out of 1.32×10^{-4} mole of water adsorbed is lost to the vapor phase by the heating of the closed tube. At the highest pressure, at most 1.87×10^{-6} mole is lost to the vapor phase out of a total of 6.17×10^{-4} adsorbed. It is therefore assumed, in the following, that the volumes listed in Table VI are the volumes of water adsorbed onto the solid in the kinetic study.

The overall decomposition of aminosalicic acid would be that

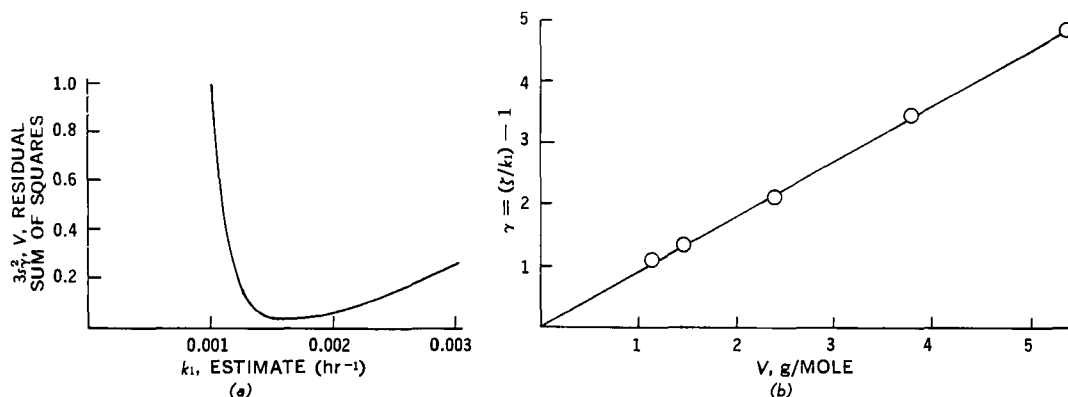
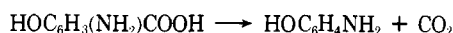


Figure 13—(a) Sum of squares of residuals for data in Tables II and V plotted versus estimate of k_1 used in Eq. 19. (b) Data from Tables II and V plotted according to Eq. 19 with an estimate of $k_1 = 0.0015 \text{ hr}^{-1}$.

of the solid and of the saturated solution if the mechanism is not diffusion controlled (24). The overall stoichiometry is the same in the solid state as in solution (Scheme II).



Scheme II

The decomposition rate constant is k_1 in the solid and k_2 in solution in the sorbed moisture layer (Fig. 11). Starting with 1 mole at time zero, there will be A' moles of aminosalicic acid left at time t ; assuming that the moisture adsorbed to the m -aminophenol is *not* part of the "available" sorbed moisture layer² means that the amount in solution is $A'VS$, where V is kilograms of water adsorbed per mole of solid, and S is solubility of aminosalicic acid in the liquid layers in moles per kilogram of water. The amount of solid aminosalicic acid present is $A' - A'VS$. The decomposition rate then is given by:

$$-\frac{dA'}{dt} = k_1(A' - A'VS) + k_2A'VS \quad (\text{Eq. 17})$$

The solution to this equation is:

$$\ln A' = -k_1 t + [(k_2/k_1) - 1]VS t \quad (\text{Eq. 18})$$

Denoting the slope of a plot of $\ln A'$ versus t by $-\zeta$, i.e.:

$$\gamma = (\zeta/k_1) - 1 = [(k_2/k_1) - 1]VS \quad (\text{Eq. 19})$$

it is clear that a plot of γ versus V should give a straight line through the origin. The data from Fig. 2 are plotted according to Eq. 18 in Fig. 12, and linearity is good in all cases.

The value of k_1 is not necessarily identical to β_0 ; the moisture present on the surface may well dissolve the active sites. This is akin to the etch test for quantitative determination of numbers of dislocations on the surfaces of metals. These dissolve more rapidly and, therefore, by short exposure to acid, leave an etch mark. If the active sites are dissolved, the nucleation would be interfered with, leading to a smaller value for k_1 than for β_0 (although, in the presence of moisture, the overall decomposition rate is increased).

By denoting the quantity $[(k_2/k_1) - 1]S$ by a , Eq. 19 has the form $\gamma = aV$. By using different values of k_1 to evaluate γ , different values of a will result. The least-squares fit formula $a = \Sigma \gamma V / \Sigma V^2$ was used; the residual sum of squares was computed for each estimate of k_1 and is shown graphically in Fig. 13a. It is obvious that the minimum in the sum of squares plot is for $k_1 = 0.0015 \text{ hr}^{-1}$, i.e., about one-half the value of β_0 . The data plotted according to Eq. 19 by this estimate of k_1 are shown in Fig. 13b.

² If all the moisture is assumed to be available, then the expression:

$$\ln [(A' + \gamma)/(1 + \gamma)] = -k_1 t$$

is arrived at. This equation gives a poorer fit than Eqs. 18 and 19.

The slope of this best least-squares fit is 0.9×10^3 moles/liter, i.e.:

$$[(k_2/0.0015) - 1]S = 0.9 \times 10^3 \quad (\text{Eq. 20})$$

It is, therefore, possible to calculate the solubility of aminosalicic acid in water at 65° from a known value of k_2 (Table VI). The calculated values bracket the value found from the solid kinetic data; the data, hence, are not incompatible with the sorbed moisture theory of Leeson and Mattocks (1).

The average surface area per mole during a decomposition is $6.141 \times 10^4 = 8.5 \times 10^6 \text{ cm}^2$. Noting that the largest moisture volume adsorbed is 5.3 ml and that, therefore, the moisture layer is at most $5.3/(8.5 \times 10^6) \text{ cm} = 62 \text{ \AA}$ thick, it follows that there is at most 15 "layers" of moisture involved. This degree of moisture coverage is considerably smaller than that in previous investigations (1, 2); this has been done deliberately to achieve a moisture coverage more in line with what might be expected in a dosage form.

APPENDIX

In Eq. 10 the following substitutions are made:

$$\begin{aligned} (\alpha_0 + \beta_0)(t_0 - q) &= m \\ u &= t - q \quad (du = dt, t = u + q) \end{aligned}$$

followed by:

$$z = \beta_0 u \quad (dz = \beta_0 du)$$

This gives:

$$dx = \{(k' \times Q)(e^{-z/a})[\beta_0^{-m+1}]\}(z^m)(e^{-z})dz = M(z^m)(e^{-z})dz \quad (\text{Eq. A1})$$

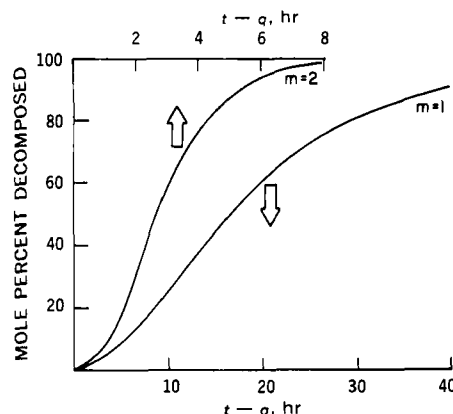


Figure 14—Theoretical decomposition curves according to Eq. A4 with $m = 1$ and $m = 2$ and $\beta_0 = 0.1 \text{ hr}^{-1}$.

Table VI—Solubilities of Aminosalicic Acid (molal) at 65° Calculated from Eq. 20 Using Reported Values of Solution Decomposition Rate Constant (k_2 , hr⁻¹)

k_2 , hr ⁻¹	Reference	Solubility (Molal) from Eq. 20
1.99	21	0.68
0.95	23	1.42
>1.14	This study	<1.19

where $M = (k')(Q)(e^{-\beta_0 q})[\beta_0^{-(m+1)}]$ is used for convenience. If Eq. A1 is integrated from $t = t_0$ (or prior times) to infinity, $x = 1$ (total decomposition); $t_0 > q$, so the integration yields unity if carried from q to infinity; if $t = q$, $u = z = 0$, so integrating Eq. A1 from $z = 0$ to infinity gives:

$$1 = M \int_0^\infty (z^m)(e^{-z})dz = \Gamma(m + 1) \quad (\text{Eq. A2})$$

so:

$$M = \Gamma^{-1}(m + 1) \quad (\text{Eq. A3})$$

where $\Gamma(m + 1)$ is the γ -function evaluated at $m + 1$. Equation A1, by partial integration, can be shown to have the general solution:

$$x = 1 - \left(e^{-\beta_0(t-q)} \sum_{i=0}^m [\beta_0(t-q)]^{m-i} [m!/(m-i)!] \right) \quad (\text{Eq. A4})$$

when m is an integer. Examples of these types of curves, showing the typical S-shape, are shown for $m = 1$ and $m = 2$ in Fig. 14.

From Eq. 2 it is seen that the inflection point of these curves occurs when:

$$d^2x/dz^2 = 0 = M(e^{-z})[z^{m-1}](m - z) \quad (\text{Eq. A5})$$

i.e., when $z = \beta_0(t - q) = m$.

REFERENCES

- (1) L. Leeson and A. Mattocks, *J. Amer. Pharm. Ass., Sci. Ed.*, **47**, 329(1958).
- (2) S. Kornblum and B. Sciarrone, *J. Pharm. Sci.*, **53**, 935(1964).

- (3) J. T. Carstensen, *ibid.*, **63**, 1(1974).
- (4) E. Garrett, *Advan. Pharm. Sci.*, **2**, 1(1967).
- (5) J. T. Carstensen, "Theory of Pharmaceutical Systems," vol. I, Academic, New York, N.Y., 1972, p. 185.
- (6) J. T. Carstensen, J. B. Johnson, W. Valentine, and J. J. Vance, *J. Pharm. Sci.*, **53**, 1050(1964).
- (7) E. G. Prout and F. C. Tompkins, *Trans. Faraday Soc.*, **40**, 488(1944).
- (8) E. G. Prout and P. J. Herley, *J. Chem. Educ.*, **37**, 643(1960).
- (9) E. Nelson, D. Eppich, and J. T. Carstensen, *J. Pharm. Sci.*, **63**, 755(1974).
- (10) K. S. E. Su and J. T. Carstensen, *ibid.*, **61**, 420(1972).
- (11) J. T. Carstensen and N. M. Musa, *ibid.*, **61**, 1112(1972).
- (12) N. M. Musa, Ph.D. dissertation, University of Wisconsin, Madison, Wis., 1972.
- (13) H. Nogami, T. Nagai, and A. Suzuki, *Chem. Pharm. Bull.*, **14**, 329(1966).
- (14) J. H. Wood, J. E. Syrato, and H. Letterman, *J. Pharm. Sci.*, **54**, 1068(1965).
- (15) K. S. E. Su, Ph.D. dissertation, University of Wisconsin, Madison, Wis., 1971.
- (16) R. T. Sanderson, "Vacuum Manipulation of Volatile Compounds," Wiley, New York, N.Y., 1948, p. 59.
- (17) P. Pothisiri, Ph.D. dissertation, University of Wisconsin, Madison, Wis., 1974.
- (18) V. Kohlschütter, *Kolloid.-Z.*, **56**, 1169(1927).
- (19) W. E. Garner and K. Pike, *J. Chem. Soc.*, **1937**, 1565.
- (20) Y. N. Sheinker and I. V. Persyanova, *Zh. Priklad. Khim.*, **26**, 860(1953); *J. Appl. Chem. USSR (English Translation)*, **26**, 783(1953).
- (21) E. Ermer, *Pharm. Ztg.*, **113**(24), 855(1968).
- (22) F. Thoma, *Tuberculosearzt*, **16**, 362(1962).
- (23) A. M. Liquori and A. Ripamonti, *Gazz. Chim. Ital.*, **85**, 589(1955).
- (24) J. T. Carstensen, "Theory of Pharmaceutical Systems," vol. II, Academic, New York, N.Y., 1973, p. 319.

ACKNOWLEDGMENTS AND ADDRESSES

Received April 23, 1974, from the School of Pharmacy, University of Wisconsin, Madison, WI 53706

Accepted for publication July 17, 1974.

Abstracted in part from a dissertation submitted by P. Pothisiri to the University of Wisconsin in partial fulfillment of the Doctor of Philosophy degree requirements.

* To whom inquiries should be directed.